

TRANSLATING BETWEEN THE SURFACE AND SUBSURFACE:
COMPARISON OF STRATIGRAPHIC AND PALEO-TOPOGRAPHIC STATISTICS

A THESIS

SUBMITTED ON THE TWENTY-SECOND DAY OF FEBRUARY 2017
TO THE DEPARTMENT OF EARTH AND ENVIRONMENTAL SCIENCES

IN PARTIAL FULFILLMENT OF THE REQUIREMENTS
OF THE SCHOOL OF SCIENCE AND ENGINEERING

OF TULANE UNIVERSITY FOR THE DEGREE OF

MASTER OF SCIENCE

BY

WILLIAM MATTHEW BENSON

APPROVED: _____

Kyle M. Straub, Ph.D., Director

Nicole M. Gasparini, Ph.D.

Torbjörn E. Törnqvist, Ph.D.

ABSTRACT

Recent work demonstrates differences between channelized topography and resulting stratigraphic surfaces at various spatial resolutions, however, at present we lack a description of how channel mobility influences this architecture. Our goal is to develop a quantitative understanding of how information pertaining to paleo-topography and morphodynamics is stored in stratigraphy. To better understand the role of channel mobility in transferring topographic information into stratigraphy we examine three physical deltaic experiments, a key difference between each being the inclusion and amount of a polymer. The polymer enhances sediment cohesion and promotes channelization from subcritical Froude number flows. To quantitatively compare topographic and stratigraphic surfaces, we measure the decay of mean absolute surface slope as a function of measurement window. In all experiments we observe steeper average slopes in the stratigraphy compared to the topography over length scales less than a channel width. The difference between stratigraphic and topographic average mean slope is the least pronounced in the weakly cohesive experiment, which is associated with the highest channel mobility. As cohesion increases and channel mobility decreases, the difference between the slopes increases. In all experiments, stratigraphic and topographic statistics converge at a length scale approximately equal to one channel width. These results suggest that channel mobility, influenced by sediment cohesion, strongly influences the storage of paleo-topographic information in stratigraphy. Specifically, we predict that systems with low channel mobility, such as vegetated river deltas, have the greatest difference in topographic and stratigraphic statistics, while this difference is minimized in high mobility systems, such as alluvial fans.

TRANSLATING BETWEEN THE SURFACE AND SUBSURFACE:
COMPARISON OF STRATIGRAPHIC AND PALEO-TOPOGRAPHIC STATISTICS

A THESIS

SUBMITTED ON THE TWENTY-SECOND DAY OF FEBRUARY 2017

TO THE DEPARTMENT OF EARTH AND ENVIRONMENTAL SCIENCES

IN PARTIAL FULFILLMENT OF THE REQUIREMENTS

OF THE SCHOOL OF SCIENCE AND ENGINEERING

OF TULANE UNIVERSITY FOR THE DEGREE OF

MASTER OF SCIENCE

BY

WILLIAM MATTHEW BENSON

APPROVED: _____

Kyle M. Straub, Ph.D., Director

Nicole M. Gasparini, Ph.D.

Torbjörn E. Törnqvist, Ph.D.

© Copyright by William Matthew Benson, 2017

All Rights Reserved

ACKNOWLEDGMENTS

I would like to extend my gratitude to my advisor Professor Kyle M. Straub for his patience, life advice, and academic guidance. He is a meticulous scientist, critical editor, and a great man. I will be forever grateful for the countless hours, funding, and ideas he has dedicated to me over these last years. Without his contributions, this project would not have been possible.

Working with the Tulane Sediment Dynamics and Quantitative Stratigraphy group has unquestionably made me a better scientist, and without their support the data collection for my thesis would have been impossible. I would especially like to thank Qi Li, Christopher Esposito, Yinan Wang, Jennifer Kuykendall, Diana Di Leonardo, Katie Pennuto, and Anjali Fernandes for their help conducting the delta experiments, collecting physical stratigraphic slices, and collecting data from the experiments and stratigraphy.

I would like to thank the students and faculty of the Tulane Earth and Environmental Sciences Department. I appreciate the support and ancillary education I received from my fellow graduate students. Specifically, I would like to thank Jordan Adams with help coding and editing my thesis. I also appreciate the opportunity to round out my previous geologic education with a variety of coursework. I would like to especially thank Professor Torbjörn E. Törnqvist and Professor Nicole M. Gasparini for serving my thesis committee.

I gratefully acknowledge support by National Science Foundation grant OCE-1049387. I would also like to acknowledge funding support by GSA graduate student research grants. Lastly, I want to thank my friends and family for their support, bringing me early morning coffee after overnights in the lab, and continued encouragement.

TABLE OF CONTENTS

ACKNOWLEDGEMENTS	ii
LIST OF TABLES	iv
LIST OF FIGURES	v
Chapter	
1. INTRODUCTION	1
2. EXPERIMENTAL METHODS.....	7
3. RESULTS	12
4. DISCUSSION.....	23
5. CONCLUSION.....	30
LIST OF REFERENCES	46

LIST OF TABLES

Table 1. Experimental Forcing Conditions

Table 2. Channel Length Scales and Mobility

LIST OF FIGURES

- Figure 1.** Schematic diagram of Tulane Delta Basin set up for the TDB-12 and TDB-13-S2 experiments featured in this thesis.
- Figure 2.** Grain size distribution used in the cohesive experiments.
- Figure 3.** Physical stratigraphy of the highly cohesive delta at the proximal transect.
- Figure 4.** Overhead photographs of the three experiments.
- Figure 5.** Physical and synthetic stratigraphic panels from experiments TDB-12 and TDB-13-S2.
- Figure 6.** Physical and synthetic stratigraphic panels from experiment TDB-10-1.
- Figure 7.** Method for measurement of slope as a function of measurement window.
- Figure 8.** Normalized count of slope measurements as a function of normalized window size for topographic surfaces.
- Figure 9.** Mean absolute slope of topographic surfaces as a function of window size in dimensional and nondimensional space.
- Figure 10.** CDF of elevation deviations from the mean.
- Figure 11.** Normalized count of slope measurements as a function of normalized window size for physical stratigraphic surfaces.
- Figure 12.** Mean absolute slope of stratigraphic surfaces as a function of window size in dimensional and nondimensional space.

Figure 13. Data defining the reduction locations along the proximal transects that have not experienced measureable topographic change.

Figure 14. Normalized value of channel mobility for the weakly cohesive, moderately cohesive, and highly cohesive experiments.

Figure 15. Mean absolute slope of physical stratigraphic surfaces, and topographic surfaces as a function of normalized window size.

1. INTRODUCTION

A river, through preserved deposition, leaves a record of its past in stratigraphy. Over intermediate geologic time periods, such as an avulsion time scale, this record is almost always incomplete due to intermittent periods of erosion or stasis (Sadler, 1981). Channelized stratigraphy therefore is at once a tantalizing inversion problem and a key to understanding Earth history. Outside of academia, channelized stratigraphy is studied to better understand potential petroleum systems. The petroleum industry has long invested in research to better understand channelized stratigraphy, but there is progress to be made in addressing stratigraphic heterogeneity.

Surfaces within outcrop or seismic data are often used to describe stratigraphy. However, what these surfaces represent within the context of channelized deltaic stratigraphy remains unclear. Are these surfaces a snap shot in time of paleo-topography or time transgressive? How are topographic surfaces tied to stratigraphic surfaces? How might variation in channel mobility affect this relationship? Motivated by these questions, the goal of this project is to address a portion of this gap in stratigraphic understanding by relating topographic and preserved stratigraphic surfaces quantitatively.

1.1 THE CHANNELIZED STRATIGRAPHIC RECORD

The stratigraphic record of paleo-channelized environments is constructed of depositional bodies separated by stratigraphic surfaces. Stratigraphic surfaces are those preserved within stratigraphy, relatively laterally continuous, that separate sediments of different grain size, mineralogy, shape, or orientation, whereas topographic surfaces refer

here to the topography of the Earth's surface at a given period of time. The disconnect between channelized topographic and stratigraphic surfaces is qualitatively discussed in previous work as some function of channel belt width and thickness, floodplain width, spatial variation of channel belt and overbank deposition rate, avulsion frequency, and intrabasin tectonics (e.g. Mackey and Bridge 1992; Bridge and Mackey, 1993a,b; Mackey and Bridge, 1995; Bryant et al., 1995; Gibling, 2006). Given these controls, it is only under special circumstances that alluvial architecture mirrors a channel pattern in a channel belt at any one point in time (Bridge, 1993).

The link between stratigraphic surfaces and paleo-topography has been examined in previous studies, including those focusing on the products of both allogenic forcings and autogenic processes. Here we refer to allogenic forcings as changes to the boundary conditions of a system, while autogenics refers to processes internal to a transport system that occur even when boundary conditions are kept constant (Beerbower, 1964; Galloway, 1971; Posamentier et al., 1988). For example, Strong and Paola (2008) note that systems experiencing large allogenic forcings (i.e. more than a channel depth of sea level fluctuation), amalgamate topographic surfaces that are both qualitatively and statistically different from the resulting preserved stratigraphic surfaces, a point also made by Li et al. (2016). As part of their study, Strong and Paola (2008) conducted an experiment which formed valleys as the result of cycles in relative sea level. However, the resulting stratigraphic valleys did not represent any instantaneous paleo-topographic surface due to valley deepening which dominantly occurred during base level fall and widening that happened during both base-level rise and fall. Similar theory for the generation of paleo-valleys has also been developed from outcrop observations

(Holbrook, 1996; Holbrook, 2001). The issue of diachronous surfaces has also been addressed for shorter time scale autogenic processes. Sheets et al. (2008) demonstrate that channel surfaces in stratigraphy are often time transgressive, formed by mobile channels, which create preserved sand bodies larger than the individual channels that crafted them. While different in scale, they did find that the aspect ratio of channel bodies and the topography of channels with scouring flow were similar. Their findings imply surfaces observed in channelized stratigraphic sections do not necessarily represent snapshots in time.

Other work demonstrates that stratigraphy has a limited memory; surficial events can be quickly erased from the record by subsequent events. Therefore, constant aggradation is required to store most topographic information (Ganti et al., 2013). Examining the relationship between topography and stratigraphy at the dune scale, Ganti et al. (2013) linked surface statistics of preserved cross set stratigraphic boundaries with the migration rate of bed forms. Specifically, they found that the local slope of stratigraphic boundaries is equal to the ratio of the bed form deformation rate to the migration rate of the bed forms in the absence of net deposition. With long-term deposition, the bed forms developed “constructed surfaces”, a composite surface composed of pieces of bed forms over time. This work advanced our understanding of bedforms and bedform stratigraphy, but we have yet to develop an equally sophisticated model for channelized deposits.

1.2 CHANNEL MOBILITY

Alluvial river channels are inherently mobile. They continuously move laterally by building bars and cutting channel banks, and they periodically avulse, abandoning the current channel path in favor of a steeper path. Combined, manuscripts by Allen (1978) and Bridge and Leeder (1979) were the first studies that quantitatively modeled the influence of channel mobility on stratigraphic architecture. Bridge and Leeder (1979) addressed how avulsions affect stratigraphic architecture in terms of the organization of channel sand bodies, while Allen (1978) addressed how the volume of overbank deposits relative to channel deposits affect alluvial architecture. Other work has furthered this understanding by incorporating field, numerical and physical experiment data to better understand how channel mobility affects the resulting stratigraphy (Mackey and Bridge, 1995; Karssenberg and Bridge, 2008; Martin et al., 2009). At present, we understand that the amount of lateral mobility a channel possesses varies with sediment flux, mean sediment grain size, the distribution of grain size, vegetation, climate, and the cohesiveness of the sediment (e.g. Blum and Törnqvist, 2000; Dunne et al., 2010; Edmonds and Slingerland, 2010; Tal and Paola, 2010). Focusing on cohesion, channel bank stabilization due to vegetation or deposit mineralogy and grain size decreases the lateral sediment flux, and helps bind levee banks together, thus stabilizing channels (Edmonds and Slingerland, 2010; Tal and Paola, 2010; Wickert et al., 2013).

Early attempts at modeling stratigraphic architecture through a channel mobility framework were focused on avulsion dominated mobility, but did not link stratigraphic surfaces with topographic surfaces (Allen, 1978; Leeder, 1978; Bridge and Leeder, 1979). Subsequent models further developed our understanding of lateral variability within fluvial systems, but stopped short of including lateral channel mobility outside of

avulsions (Mackey and Bridge 1992; Bridge and Mackey, 1993a,b; Bryant et al., 1995; Mackey and Bridge, 1995). Here, we define channel mobility as the sum of channel movement associated with gradual lateral translation plus infrequent punctuated relocation through avulsion. This definition is similar to one recently proposed in equation form by Wickert et al. (2013).

A framework for quantifying the dominant style of channel mobility, ranging from slow lateral migration to punctuated avulsion, was proposed by Jerolmack and Mohrig (2007). In this study they compared the time to aggrade a channel by one channel depth to the time required to laterally migrate a channel by one channel width. In this case, it was found that as the ratio favored aggradation, and thus mobility through avulsion, several channels were generally active at once. As the ratio favored lateral incision, and thus mobility through gradual translation, they hypothesized there would generally be a single channel rapidly sweeping across the flood plain, leaving behind channel belts in stratigraphy (Jerolmack and Mohrig, 2007).

Little work has been done to quantify the mobility of an entire fluvial system because of the long time scales and large preserved areas required. This is necessary to test the proposed controls on channel mobility mentioned earlier and will require either large field scale campaigns and/or physical experiments.

1.3 STUDY GOALS

This project will analyze the link between channelized stratigraphic surfaces and paleo-topography. We will focus on stratigraphic surfaces that were never topographic surfaces or as defined by Strong and Paola (2008); “surfaces that never were”. While previous studies have limited their analysis to channelized surfaces (Sheets et al., 2008), we will examine all stratigraphic surfaces in channelized stratigraphy (i.e. surfaces in channel, and floodplain facies).

Armed with the aforementioned understanding of channel mobility, we aim to address how varying levels and types of channel mobility affect the stratigraphic record of channelized deltaic settings. Using data from physical experiments, we quantitatively address differences in topographic and stratigraphic surfaces as a function of channel mobility. We aim to define a basin averaged channel mobility following a similar normalization as that of Jerolmack and Mohrig (2007), but focus on basin averaged properties, rather than the properties of a single channel. This will be done through a normalized comparison of delta aggradation rates (both channel and non-channel) to a lateral reworking time scale of an entire delta top. We hypothesize that differences in spatial statistics, such as slope, between topographic and stratigraphic surfaces is a function of channel mobility. We expect for systems experiencing constant forcings, the spatial resolution at which spatial statistics for stratigraphic and topographic surfaces converge is equivalent to one channel width. In the subsequent section, methodology related to three physical fluvial-deltaic experiments, associated data collection and processing are discussed. The surface statistics collected from the experiments are then

compared for similarity between topographic and stratigraphic surfaces based upon relative channel mobility.

2. EXPERIMENTAL METHODS

To examine the transfer of topographic information to the sub-surface, we explore results from three physical experiments that vary in lateral mobility. In this thesis we will refer to a normalized lateral mobility, a measure of a system's lateral mobility to long term aggradation rate. In addition to exploring a range of normalized lateral mobility, the experiments varied in their ratio of bedload to suspended load. We hypothesize that these ratios fundamentally influence the link between topographic and stratigraphic surface statistics in channelized autogenic settings.

We explore the link between topographic and stratigraphic surfaces with physical experiments for the following reasons: 1) Experiments allow for direct observation of surface dynamics and their link to stratigraphic products over time scales that can encompass tens of channel avulsion cycles. 2) Experiments allow for precise control of system boundary conditions. 3) Experimental systems produce rich stochastic autogenic dynamics not found in many reduced complexity numerical models that are typically deployed for modeling generation of stratigraphy over geologic time scales, given current computing powers. While directly upscaling experimental systems to field scales remains challenging, the existence of scale independence in some aspects of sediment transport and morphodynamics allow experimental systems to produce spatial structure and kinematics that, although imperfect, compare well with natural systems (Paola et al., 2009).

In addition to a previously conducted experiment, two new experiments were performed for this study, which were conducted in the Delta Basin at Tulane University's Sediment Dynamics Laboratory (Figure 1). The basin is 2.8 meters wide by 4.2 meters long by 0.65 meters deep. Accommodation space is created in the Delta Basin by increasing base level utilizing a motorized weir that is in hydraulic communication with the basin. This system allows base-level control through a computer interface with submillimeter resolution. Water and sediment supply to the basin are also controlled through the computer interface, and were kept constant throughout each experiment. During all stages, sediment and water were mixed in a funnel and fed from a single point source. Both experiments began with an initial stage with no relative subsidence. After a system prograded to a desired delta top area, the main experimental stage began. During this stage, base level increased at a rate equal to the total sediment discharge rate divided by the desired delta-top area. As a result, the combination of sediment feed rate and base-level rise allowed the delta top area to be maintained at an approximately constant size through the course of the main stage of each experiment. These two new experiments had identical infeed rates of water and sediment and base level rise rates. Table 1 details data pertaining to system boundary conditions in these experiments.

An innovation in physical experiments enables the formation of deltas with strong channelization at sub-critical Froude numbers through use of a sediment mixture that includes an artificial polymer (New-Drill Plus, Baker Hughes Inc.) (Hoyal and Sheets, 2009). The enhanced cohesion provided by the polymer mimics the effect of vegetation and dewatered clays at reducing channel mobility. This sediment mixture, devised by Hoyal and Sheets (2009), allows for the formation of levees and overbank deposits. Here

we deploy a modified version of the Hoyal and Sheets (2009) sediment mixture (Figure 2), with varying concentrations of polymer to influence system cohesion and thus lateral mobility. Similar to Hoyal and Sheets (2009), our mixture includes a wide distribution of grain sizes, ranging from 1-1000 μm . The first experiment, termed TDB-12, was designed to be highly cohesive and included 80 grams of polymer per 120 lb batch of sediment. The second experiment, termed TDB-13-S2, was designed to be moderately cohesive and included 40 grams of polymer per 120 lb batch of sediment. Differences in channel dynamics drove differences in deltaic sediment retention in the two experiments. As a result the average delta top areas differed in the two experiments, with the moderately cohesive TDB-13-S2 having the larger average delta-top area (Table 1). The two experiments also differed in their total run time. The highly cohesive TDB-12 ran for 900 hours, while TDB-13-S2 ran for 700 hrs. While run time varied, each experiment aggraded a sediment package at least 10 times their mean channel depth.

To complement our new results and explore systems with different absolute boundary conditions, we examine data from a previously reported upon experiment, TDB-10-1 (Wang et al., 2011). The experiment was conducted in the Tulane Delta Basin, but with the sediment and water infeed centered on one of the 2.8 meter basin walls and with an entrance box that expanded outward to the side walls. With this design, the delta filled the entire 2.8 m width of the basin, prograded 3.1 m from source to shoreline, and aggraded 0.415 m over the course of the experiment. This weakly cohesive experiment utilized a sediment mixture comprised of 70% by volume quartz sand ($D_{50} = 110 \mu\text{m}$) and 30% anthracite sand ($D_{50} = 440 \mu\text{m}$). The anthracite sand has a specific gravity of 1.3, and the quartz has a specific gravity of 2.65. While larger than the

quartz sand grains, the anthracite sand is significantly more mobile than the quartz sand due to its lower specific gravity and serves as a proxy for fine-grained clastics. Sediment and water discharge in this experiment were much greater than the new moderately and highly cohesive experiments, as was the background base level rise rate (Table 1). The higher feed rates in the lower cohesion experiment generated a system that evolved over shorter time scales than our two increased cohesion experiments and as such the experiment only lasted 80 hrs. Similar to the increased cohesion experiments, though, this was enough time to generate in excess of 10 channel depths worth of stratigraphy.

Topography of the experimental surfaces for the highly and moderately cohesive experiments was collected using a 3D Laser Scanning system to generate digital elevation models (DEMs) once an hour. These DEMs have a grid spacing of 5 mm in the down and cross basin directions and have a vertical resolution of 1 mm. For the highly cohesive experiment, additional topographic transects were collected from the experimental surface using orthographic photographs of sheet lasers, once an hour at strike transects 0.89 and 1.35 m downstream of the basin entrance (Figure 1). The topography of the weakly cohesive experimental surface was recorded using sheet lasers and orthographic photographs at 2 minute intervals along three flow-perpendicular transects, located 1.63 m, 2.1 m, and 2.6 m from the infeed point. The sheet laser topographic lines have a horizontal grid spacing of 1 mm and vertical resolution of 1 mm. The temporal resolution for each experiment was sufficient to capture the meso-scale dynamics. In addition to elevation, the DEMs collected with the 3D Laser Scanner include information on color. Similar to a digital camera, the 3D scanner collects information on the intensity of the red, blue, and green color channels. In the highly and

moderately cohesive experiments, 5% of the sediment mixture, a quarter of the 20% coarsest fraction, is composed of colored sediment, so the color information can display spatial locations of coarse grained deposits. Digital photographs were also collected at a 15 min interval during the highly and moderately cohesive experiments and every 1 min of the weakly cohesive experiment, with dye introduced to the input flow to further document system morphodynamics.

To ground truth DEM based surfaces, the physical stratigraphy of the delta was also analyzed. Physical stratigraphy was sampled using a metal wedge filled with dry ice and methanol which was inserted into the deltas along transects 0.89 m and 1.35 m from the source, while the delta was submerged in water (Figure 3). The dry ice and methanol lowered the temperature of the metal wedge to -70° C. This low temperature froze the water within the pore spaces of the deposit close to the wedge, binding the sediment together in order to extract the preserved stratigraphy from the delta. These stratigraphic transects were then photographed using digital cameras. The digital photographs are converted into grayscale and the visualization of the colored coarse sediment, which is dark relative to the majority of the mixture, is enhanced by increasing the contrast of the images. The grayscale image is then converted to a standard seg-y data format for import to a seismic interpretation package where all visible bed boundaries are mapped. In this way, it is similar to mapping impedance contrast boundaries in seismic data, which can be the result of changes in grain size.

3. RESULTS

Observations of surface dynamics as the deltas aggraded, and collected stratigraphic panels reveal three similar yet distinct deltaic systems. The surface dynamics of all three deltas followed a pattern of autogenic channel formation, followed by back stepping, and avulsion. This process occurred over longer time scales as cohesion was increased in the three experiments (Figure 4). With increases in sediment cohesion, there were noted decreases in channel mobility and increases in shoreline variability. As cohesion increased the stratigraphic architecture of the deltas became characterized by both levee and overbank deposits (Figures 5 and 6). All three physical stratigraphic panels are dominated by channel fill deposits.

3.1 SURFACE STATISTICS

We are interested in measuring how channel mobility influences the structure of stratigraphic surfaces and how these surfaces compare to topography. To address this problem, we examine topographic, and physical stratigraphic surface statistics along strike cross-sections of our experiments (Figures 5 and 6). We use strike transects due to approximately equivalent environments of deposition found across strike as opposed to a dip sections. In particular, we use a strike transect 0.89 m from the entrance channels for the cohesive deltas, and a corresponding cross-section located 1.63 m from the entrance condition for the weakly cohesive delta. In mass balance space, the transect for the highly and moderately cohesive deltas is located radially, ranging between the center of the stratigraphic slice where 20% of the sediment is stored upstream, and at the edges of the stratigraphic slice where 35% of the sediment is stored upstream (Li, 2016). The

physical stratigraphy transect for the weakly cohesive delta is located at a location where 43% of sediment is stored upstream (Straub and Wang, 2013). It is therefore possible that differences between the more cohesive deltas and the weakly cohesive delta can be attributed to the different locations in mass balance space. Nevertheless, these strike locations correspond to settings with well-developed channels, while also being a significant distance away from their entrance condition to minimize boundary effects. Topography along these transects are processed to interpolate missing data, as well as remove data points from bad reflections or errant material floating on the water.

A first order characteristic of a surface is its slope. Across many scales and in many environments, surface slopes influence morphodynamics, and are an important aspect of how we analyze stratigraphy (e.g. Niemann et al., 2001; Ganti et al., 2013). The slope of a topographic surface influences, amongst other things, the amount of solid and fluid mass that can be transferred over a given region, the stability of a surface, and the ecology of a setting (Kim et al., 2006; Kim and Paola, 2007; Kim and Jerolmack, 2008; Tal and Paola, 2010). The slope of a stratigraphic surface is known to be influenced by paleo-topography and its mobility, in addition to rates of vertical aggradation (Strong and Paola, 2008; Hoyal and Sheets, 2009; Straub et al., 2013).

In many fluvial-deltaic settings, the average slope along a given strike transect is approximately zero. While features with high slopes generally exist, they often are canceled out by features with similar magnitude, but opposite sign somewhere else along the transect. For example, high slopes along one channel bank are canceled out by the slopes on the opposing bank due to the symmetrical nature of channels (Figure 7). As we are interested in the general magnitude of surface slopes, and not necessarily the sign, we

examine the mean absolute value of slope $\overline{|s|}$ and how it changes as a function of measurement window.

Measurements of slope are generally length scale dependent, which has been explored in studies of the Earth's surface (Mark and Aronson, 1984; Niemann et al., 2001). This past work has established that there are critical length scales over which slopes can be predictably modeled based upon available data. As the length over which a slope is being measured increases, it becomes less representative of the local slopes occurring below the threshold of the ruler length. This phenomenon will occur across all scales, as the rugosity of interest for a system can only be recorded if it is measured by a ruler smaller than the changes in elevation. To examine this phenomenon in deltaic settings we explore how $\overline{|s|}$ changes as a function of measurement window size. Every continuous surface is measured for absolute slope for every possible window size (dx), where x is a measure of a cross-stream distance in the basin. For a given dx of interest we calculate $\overline{|s|}$ with the following equation:

$$\overline{|s(dx)|} = \frac{\sum_{j=1}^{N_s} \sum_{i=1+dx/dx_{min}}^{L_j/dx+1} \left| \frac{\eta_{j,i} - \eta_{j,i-dx/dx_{min}}}{dx} \right|}{\sum_{j=1}^{N_s} \left(\frac{L_j}{dx_{min}} + 1 \right) - \frac{dx}{dx_{min}}} \quad (1)$$

where N_s is the number of surfaces analyzed which are at least dx in length, L is the maximum length of a surface, dx_{min} is the smallest possible discretization in the x direction and η is a measurement of elevation. A graphical description of the application of equation 1 is shown in Figure 7.

When plotting values of mean absolute slope ($\overline{|s|}$), we concern ourselves with the measurement windows over which we have statistical significance. For all surfaces, as window size increases, the number of observations decreases. This occurs because the recorded surfaces are a fixed length, while the length scale over which slope is measured increases (Figure 8). In our analysis, we normalize the recorded number of elevations for a given dx by the maximum number of measurements collected for the smallest window size for each experiment. In all experiments, the topographic surfaces have the largest number of measurements at the smallest window size. We choose to limit our analysis of $\overline{|s|}$ window sizes in the smallest 95% of measurement windows. This decision was made because the number of observations at very large window sizes is small enough to be influenced by outlier values of slope.

For the topography of all experiments, $\overline{|s|}$ declines with increasing dx towards the basin averaged value, 0, following an approximately exponential decay (Figure 9). In the weakly cohesive experiment, we also observe a regime over smaller window sizes where $\overline{|s|}$ remains approximately constant with increasing dx . We do not see a similar regime in the more cohesive experiments as the horizontal spacing between measured elevations was greater than in the weakly cohesive experiment and due to the capability for the cohesive sediment mixtures to maintain near vertical slopes prior to failure. Finally, we observe higher $\overline{|s|}$ for a given window size in the two cohesive experiments, compared to the weakly cohesive experiment.

These results can be nondimensionalized, so that systems of varying scales can be compared and contrasted. As slope is already nondimensional, we only need to address our horizontal length scales. Ideally, we would attempt this nondimensionalization using a fundamental length scales of rivers, for example either their width (B) or depth (H_c). Channels can be identified from over-head photographs, however, these do not provide information on their depths. Using DEMs, elevation differences can be seen, but these do not provide information on whether or not a local minimum in elevation is an active channel. Due to the difficulties in measuring channel depths directly, we use a proxy for H_c that characterizes the roughness of the topography. We specifically focus on a length scale that has been shown to correspond to the largest channels in systems with constant boundary conditions. We estimate the maximum roughness length scale (l) as the 97.5 percentile of the cumulative density function of elevation (CDF) minus the 2.5 percentile of the CDF (Figure 10 and Table 2) (Li, 2016). The 50th percentile represents the average elevation along the strike transect and typically corresponds to the elevation of floodplains. The 2.5 percentile is a scale which typically corresponds to the bottom of channels along a transect, while the 97.5 percentile is a scale which typically corresponds to the crests of levees. The difference between the 97.5 and 2.5 percentiles of the detrended elevation CDF is therefore representative of a maximum channel depth.

Channel widths of the weakly cohesive delta were measured from the overhead photographs as the average wetted width of individual flow threads in all measured transects. Channel widths in the weakly cohesive delta were measured this way as all flow threads were associated with active channelized sediment transport by bedload. The channel widths of the moderately and highly cohesive deltas were measured by hand

along each transect of interest using overhead digital photos. This was necessary to capture the full extent of the channel widths, as both experiments experienced both channelized and overbank flow.

The $\overline{|s|}$ trends of the topographic data set discussed above for the non-normalized window sizes remain true once window size is normalized. This is true regardless of whether the normalization is done with B or H_c (Figure 9B and 9C). Notably, when normalizing window size by H_c , the curves converge at approximately 10 channel depths. Once converged, the curves track together as the ratio dx/H_c increases.

3.2 STRATIGRAPHY

Images of the physical stratigraphy from the three experiments reveal strong difference in stratigraphic architecture. As most sediment transport in the weakly cohesive experiment occurred as bedload, many high curvature erosional channel surfaces are present in the stratigraphy, in addition to lower curvature surfaces deposited by sheet flow over terminal lobes. In contrast, the stratigraphy resulting from the moderately and highly cohesive experiments included high curvature channel features, some erosional, but mostly aggradational. Further, the more cohesive experiments included levees and surfaces interpreted to be the result of overbank deposition in floodplains.

Using the surfaces mapped from the physical stratigraphic panels, we characterize a similar set of surface statistics for the stratigraphy as was done for topography. In comparison to the topographic surfaces, the percent of observations is compressed to the

smaller measurement windows in the stratigraphic data set (Figures 8, and 11). There is an order of magnitude decrease in the size of measurement windows with usable data.

Similar to our topographic surface analysis, we present $\overline{|s|}$ of the stratigraphic surfaces against dimensional window size, in addition to window sizes normalized by both B and l (Figure 12). The observed trends are similar in basic structure to the corresponding topographic plots, with the magnitude of $\overline{|s|}$ decreasing with increasing length scales. The more cohesive experiments generally have higher magnitude stratigraphic slopes over the same normalized length scales compared to the weakly-cohesive experiment. In contrast to the topographic surfaces, where the two more cohesive experiments shared similar $\overline{|s|}$, there is clear reduction in the stratigraphy $\overline{|s|}$ from the highly cohesive to moderately cohesive, to the weakly-cohesive experimental deposits (Figure 12).

A similar suite of surface statistics was generated from synthetic stratigraphy, generated from topographic transects stacked and clipped for erosion, and from synthetic erosional stratigraphy generated from preserved erosive topographic surfaces (Martin et al., 2009). Unfortunately, issues with spatial and temporal resolution resulted in us being unable to use the data.

3.3 MORPHODYNAMICS

From observations of surface dynamics, one key qualitative observation was the difference in channel mobility. A reduction of channel mobility was observed in our experiments with increasing sediment cohesion. Still images of the experiments,

displayed in Figure 4, highlight the differences in experimental surface dynamics. As channel stability increased, due to increases in cohesion, the primary building blocks of the stratigraphy changed from that of cut and fill bedload deposits (weakly cohesive image, Figure 4) to a combination of bedload and suspension fallout deposits (highly cohesive Figure 4).

Observations during the highly cohesive experiment indicated that coarse material was mostly transported as bedload in channels, while fine material was often transported in suspension, some of which constructed levee and floodplain deposits. Similar to previous experiments that used this sediment mixture, the delta top area in the highly cohesive experiment oscillated as the morphodynamics went through phases of channelization, overextension, back-stepping, and avulsion (Hoyal, and Sheets, 2009). These processes drove the distribution of sediment into elongated lobes as opposed to an evenly distributed fan.

The moderately cohesive delta developed levees, but they were smaller than those produced in the highly cohesive experiment. This experiment had similar morphodynamics to the highly cohesive experiment in that levees developed, and there was suspension fallout sedimentation. However, the morphodynamic cycles described above operated more rapidly in comparison to the highly cohesive experiment.

The weakly cohesive experiment was dominated by bedload transport. Rapid lateral spreading of the flow, induced by mid-channel bars, resulted in shallow flow thicknesses and sediment transported within several grain diameters of the bed. This means levees did not develop and the mode of sedimentation was limited to bedload transportation. The geomorphic surface was highly mobile as a consequence of the lack

of levees to confine flow. Incisional scours, formed at hydraulic jumps, were mobile and migrated rapidly over the geomorphic surface.

We quantify differences in channel mobility, used to examine controls on the difference between topographic and stratigraphic slopes. We first define a metric for channel mobility. Previous experimental studies have quantified channel mobility by tracking the amount of time necessary for flow to visit most locations in a basin (Cazanacli et al., 2002; Kim et al., 2010; Straub, and Wang, 2013). This is accomplished using overhead photos, where regions occupied by flow are differentiated from dry regions. A time series of these photos can then be used to quantify the amount of time necessary for flow to visit 95% of the delta top (Powell et al., 2012; Straub and Esposito, 2013).

We utilize a method developed by Li (2016) that tracks the amount of time necessary for 95% of the surface to experience a measurable change in elevation, indicating surface modification. We do this as our cohesive experiments had frequent non-channelized flow events that did little to alter topography or influence stratigraphic architecture. We start by creating difference maps with successive topographic surveys, which are used to identify areas of the experimental surface that underwent either 1 mm of erosion or deposition. The 1 mm threshold is used as it corresponds to the resolution of our topographic surveys. A decay curve is generated using the cumulative percent of the map having undergone at least 1 mm of elevation change measured for each future time step. This process is repeated, starting with each possible DEM that is followed by enough topographic surveys to observe 95% reworking. For each experiment, all measured decay curves are averaged, and the average number of experimental hours

associated with 95% reworking of the experimental surface is calculated. This timescale, referred to as T_{ch} , provides a measure of system mobility that incorporates morphologic change resulting from both fully channelized as well as unchannelized flow. The decay curves for the experiments are seen in Figure 13 A-D, and produce T_{ch} values of 1.1 hours, 45 hours, and 50.5 hours for the weakly cohesive, moderately cohesive, and strongly cohesive experiments, respectively (Table 2).

While T_{ch} is an adequate measure of system mobility it does not contain information with regard to how this mobility influences stratigraphy, as it does not take into account how rapidly a deposit is aggrading. To accomplish this, we seek to normalize T_{ch} by a timescale that describes the average aggradation rate of the system. This is accomplished using the time necessary to aggrade, on average, one channel depth of stratigraphy across an entire transect:

$$T_c = \frac{l}{\bar{r}} \quad (2),$$

where \bar{r} is the long term aggradation rate of a system. This timescale has been defined in previous studies for stratigraphic analysis and is referred to as a compensation time scale, T_c (Wang, et al., 2011; Straub, and Wang, 2013). Here, we calculate T_c using H_c as a proxy for l , as done in previous studies (Wang, et al., 2011; Straub, and Wang, 2013). Calculated values of T_c are 3.6 hours, 109.4 hours, and 84.9 hours for the weakly cohesive, moderately cohesive, and strongly cohesive experiments, respectively (Table 2).

A ratio of T_c to T_{ch} results in a unitless metric of deltaic system mobility, T^* . One way to view T^* is as the minimum number of times that an event which induces topographic change occurs at a site during the basin-wide aggradation of one H_c . This can

be seen by comparing two deltas which share an equivalent T_c , but varying T_{ch} . Each spot on the delta characterized by the higher T_{ch} is only infrequently modified during a period of duration T_c and has a low T^* . Conversely, each spot on the delta characterized by the lower T_{ch} will be frequently reworked during the same period and have a higher T^* . We observe that an increase in cohesion decreases the value of T^* . The T^* values for the weakly cohesive, moderately cohesive, and strongly cohesive experiments are 3.3, 2.4, and 1.7 respectively (Figure 14 and Table 2). Expressed in another way, the T^* values show that for the weakly cohesive delta most locations experience at minimum three surface modification events during the time necessary to aggrade one channel depth. Most locations on the moderately cohesive delta will experience surface modification events approximately $2\frac{1}{2}$ times as the system aggrades 1 channel depth. Surface modification events will, at a minimum, affect most locations on the highly cohesive delta top area $1\frac{3}{4}$ times as the system aggrades 1 channel depth.

4. DISCUSSION

4.1 INFLUENCE OF MORPHODYNAMICS ON STRATIGRAPHY

In order to relate our nondimensional measure of mobility (T^*) to stratigraphy we examine the relative differences between stratigraphic surfaces and topographic surfaces for each experiment (Figure 15). The largest difference in surface statistics is associated with the highly cohesive delta which is the least mobile. These differences in surface statistics are due to the large levees, and the large floodplain area relative to the other experiments. This translates to the surface statistics as steep stratigraphic surfaces, because the channels and levees are vertically aggraded leaving behind steep vertically exaggerated channel fill deposits. The floodplain deposition continuously aggraded the delta top in non-channelized locations, resulting in shallower topographic statistics relative to the moderately and weakly cohesive experiments. Additionally, the amount of floodplain deposits preserved in stratigraphy were significantly fewer than the amount recorded as topography. This is not necessarily because the floodplain deposits were eroded away, but because there was a less noticeable differentiation in grain size between subsequent floodplain deposits as compared to channel deposits. The morphodynamics of a highly cohesive system maximize the differences between surface statistics of stratigraphic and topographic surfaces because high slope channel topography is more likely to be preserved as stratigraphy compared to the accompanying low slope flood plain topography.

By comparison, the stratigraphy of the weakly and moderately cohesive experiments, which are more mobile, were characterized by discontinuous, diachronous and amalgamated surfaces. Morphodynamically, the moderately cohesive and weakly

cohesive experiments are different. The weakly cohesive experiment, in confirmation of prior studies using a similar sediment mixture, was an extremely mobile bedload dominated system with stratigraphy consisting of amalgamated sand bodies (Sheets et al., 2008; Strong and Paola, 2008; Wickert et al., 2013). Despite these differences both experiments had quantitatively similar differences between their respective stratigraphic and topographic surface statistics. Relative to the differences of the highly cohesive delta surface statistics, the differences between stratigraphic and topographic surface statistics associated with the weakly and moderately cohesive deltas are smaller.

We expected the highly mobile, weakly cohesive experiment to possess the largest differences between surface statistics of recorded topography and the resulting stratigraphy. This expectation stemmed from the understanding that the more mobile, weakly cohesive experiment would laterally migrate more often, erasing previous surfaces while leaving behind relatively steep channel deposits. However, the least mobile, highly cohesive experiment produced the largest differences between surface statistics of recorded topography and the resulting stratigraphy (Figure 15). The highly cohesive delta achieved this through less frequent aggradational channels that possessed high magnitude slopes, and contrasted the surrounding, relatively flat flood plain deposits. This suggests there is a possible threshold of mobility, below which differences in surface statistics become larger. The highly cohesive experiment likely reached this threshold, while the weakly and moderately cohesive experiments did not. In a physical sense this threshold is reached when the levees are not high enough to prevent all overbank deposition, but high enough to only allow the finest fraction of sediment to be deposited as overbank deposition.

4.2 IMPLICATIONS OF SURFACE STATISTICS

We can also examine the surface statistics for the physical stratigraphic surfaces and topographic surfaces for their similarities. The physical stratigraphic surface statistics are plotted with the topographic surface statistics for the experiments (Figure 15). We normalize the window size of slope measurement by the maximum depth of each system's channels (H_c) which was estimated as the calculated maximum roughness length scale (l) of each experiment. A dotted line is used to project the same decline rate seen in the highly cohesive stratigraphic surfaces to the intersection with the topographic curve. The dotted line is necessary because at very large window sizes there are fewer observations. This results in a greater variance in the data, and the mean deviates irregularly from its previous continuous trend, suggesting statistical insignificance. For all three experiments, the respective stratigraphic and topographic surface statistics converge near $10 H_c$ (Figure 15). Specifically, the set of surfaces converge at approximately $8 H_c$ for the weakly cohesive experiment, $7 H_c$ for the moderately cohesive experiment, and $10 H_c$ for the highly cohesive experiment. The length scale of surface statistic convergence ($10 H_c$) has been shown to be a minimum width to depth (B/H_c) ratio for field scale alluvial rivers (Rosgen, 1994). The variability in the length scale at which the topographic and stratigraphic \overline{s} curves meet could be due to differences in the width to depth ratio of the channels in each experiment, induced by varying levels of cohesion.

Increasing cohesion increases the upper bound of sustainable slopes within the delta. At the smallest measurable normalized window sizes, the magnitudes of slope are

at their highest. As slope magnitudes approach 0 the surface statistics values of the more cohesive deltas decrease, while the weakly cohesive delta experiences a rollover (Figure 15). This magnitude of slope at this rollover is likely determined by some aspect of the angle of repose for the different sediment mixtures. Adding artificial cohesion effectively increases the angle of repose for the sediment.

The $\overline{|s|}$ decay curves for both topographic and stratigraphic surfaces have similar slopes for all three experiments (Figure 15). The topographic surface statistics decay at similar rates, and the primary difference between topographic surface statistics is their y-intercept. This holds true for the stratigraphic surfaces as well (Figure 15). As mentioned above, the intercepts are likely controlled by the amount of cohesion added to the sediment mixture, effectively altering the morphodynamics of the system (T^*), and increasing the angle of repose. Despite having different sediment mixtures for the strongly and moderately cohesive experiment than for the weakly cohesive experiment, the resulting surface statistics of the experiments are comparable and follow a characteristic pattern that can be applied across disparate data sets of surface statistics (Hoyal and Sheets, 2009, Wang et al., 2011).

Physical stratigraphic surface statistics initially have a higher magnitude than topographic surface statistics, and have steeper declines. However, the physical surface statistics experience a rollover after which they all decay at similar rates in a shallower, similar pattern as the topographic surfaces (Figure 15). This suggests that cohesion, while increasing the overall magnitude of slopes, does not affect the convergence of topographic and stratigraphic surface $\overline{|s|}$ statistics at a length scale of approximately one

channel width. For our experiment, channels were the largest lateral length scale erosional feature, but in other experiments or field systems this length scale could be the largest valley incised during sea level fall, zone of uplift, or zones of subsidence (Strong and Paola, 2008; Kim et al., 2010).

4.3 FIELD APPLICATIONS

Our observation that the decays of $|\overline{s}|$ for stratigraphic and topographic surfaces converge at approximately one channel width could be useful in an outcrop setting, as there will be differences in the fidelity of the rock record when examining different systems along the mobility spectrum. Highly mobile systems, such as an alluvial fan, can be expected to possess more heavily amalgamated surfaces in stratigraphy (Reitz, et al., 2012). It is less likely that surface features in such a system would transfer into the rock record without strong modification. Such a system will behave similarly to our weakly cohesive experiment in both surface statistics and mobility metrics. On the other end of the spectrum, low mobility systems such as a vegetated river delta will have more stratigraphic surfaces that more closely resemble paleo-topographic surfaces (Tal and Paola, 2010). That type of system will behave similarly to our highly cohesive experiment in its surface statistics and mobility metrics. Knowing that the surface statistics of all systems converge at approximately the minimum channel width can aid interpretation of field data, provided the maximum roughness length scale is known. Length scales larger than the maximum roughness length scale can be used to measure stratigraphic surfaces in order to quantify aspects of paleo-topographic surfaces.

4.4 AVENUES FOR FUTURE WORK

There are many opportunities to expand upon this work in the future. An avenue worth exploring is relating surface statistics from field data to this set of results. Whether through meta-research, outcrops, or seismic data, surfaces could be generated from natural systems from along a mobility spectrum and compared with our results in order to potentially ascertain the relative amount of cohesion of the system, or potentially even critical length scales for that field system. In a field scale system subject to allogenic forcings, the length scale over which different systems could be normalized to converge would most likely not be the channel width, but the largest valley incised by the system.

Another opportunity for future work could be expanding upon the surface statistics we presented. Examining the curvature of the topographic and stratigraphic surfaces has been done in other studies could provide fruitful new insights (Ganti et al., 2013). Curvature would provide additional information on the shape of the channels in the system, and limit the influence of flat flood plain deposits that still possess a small slope. Any future work along this line of inquiry would benefit heavily from being able to quantify the direct effect of the cohesion added by the synthetic polymer on shear stress. Because the polymer reacts with varying levels of water and grain sizes, it has proven difficult for us to quantify the added amount of critical shear stress associated with varying amounts of the polymer. This metric would be highly useful in comparing our system mobility metric, T^* , in a quantitative as opposed to relative manner. This information could also be usefully applied to field scale systems in projecting the mobility of the system and relating this mobility to the surface statistics of the system.

Additional experiments incorporating allogenic changes such as sea level rise and fall could also be used to further this work and explore the critical length scales associated with those systems. As mentioned above, the roughness length scale on which the systems converge, once normalized, would be larger than a channel width. Future experiments could also benefit from higher temporal and spatial resolution which could aid in developing a better understanding of the amalgamated surfaces in stratigraphy. Numerical experiments that simulate surface dynamics, and the building of stratigraphy could also be used to quickly, and more cost-effectively test the above ideas.

Future experiments, particularly numerical ones, incorporating higher spatial and temporal resolution data could be used to generate synthetic stratigraphic surfaces, and synthetic erosional surfaces. Comparing these with the topographic and stratigraphic surfaces could generate additional insights into the fidelity of a system's stratigraphic record in representing the precedent topography. The higher resolution data set is necessary to combine the clipped temporally distant surfaces into larger surfaces more representative of stratigraphic surfaces.

Despite exhaustive efforts, it proved impossible to generate a synthetic stratigraphic volume that quantitatively reflects the physical stratigraphy in plots of surface statistics. A notable difficulty encountered in this effort was the lack of continuous erosional surfaces in the experiments containing artificially higher amounts of cohesion. This problem occurred because the moderately and highly cohesive experiments generated channels through the aggradation of channel levees created through overbank flow rather than the purely incisional channels generated in the weakly cohesive experiment. An additional noteworthy issue was determining where or if

erosional surfaces amalgamated into larger surfaces. Even with the very high temporal resolution of the data sets used in this study, it was impossible to link erosional surfaces that while sharing a high degree of spatial proximity were temporally very disparate. Due to limitations in topographic data collection, a complete record of the depositional histories of these experiments is impossible.

5. CONCLUSION

Our experimental results confirm previous work demonstrating that cohesion within a fluvial deltaic system promotes levee growth, more stabilized channels, and flows that are Froude subcritical (Hoyal and Sheets, 2009). Added cohesion shifts the morphodynamics of the delta from an alluvial fan regime towards a bird's foot-style, river dominated delta with channel patterns and irregular coastlines. Expanding upon these previous findings, increasing cohesion also decreases mobility. Part of operating with Froude subcritical flows means longer-lasting channels with changes in channel locations occurring primarily during avulsions, separated by longer periods of aggradation and meandering.

Increasing the amount of cohesion with the fluvial deltaic system also resulted in steeper average slopes over length scales less than one channel width. We attribute this outcome to increased cohesion increasing the upper bound of sustainable slopes within the delta over a constant length. Over length scales less than a channel width, increasing cohesion will allow the sediment to better bind into increasingly steeper slopes in effect increasing the angle of repose for the materials. The increased surface slopes achieved in this manner are in turn translated into steeper relative slopes once stored as stratigraphy.

The decay curve associated with the mean absolute value of slope over increasing measurement windows is steeper for stratigraphic surfaces than topographic surfaces until they converge at approximately one channel width. Within the autogenic dominated deltaic systems, we examined a channel width as the largest topographic feature. Past one channel width, there are fewer stratigraphic surfaces and they bear very similar statistics to the topographic surfaces of this length. In a field scale system, this length

scale could be expected to correspond to the largest allogenic feature such as a river valley.

Both topographic and stratigraphic surfaces experienced similarly sloped decay curves across experiments. This suggests that while cohesion increases the average sustainable slope over a certain length scale, the rate at which the average sustainable slope decreases for each type of surface remains unaffected by added cohesion. We hypothesize field scale systems with low channel mobility, such as vegetated river deltas have the greatest difference in topographic and stratigraphic statistics, while this difference is minimized in high mobility systems, such as alluvial fans.

Table 1. Experimental Forcing Conditions

Experiment	Duration (hr)	Q_w (L/s)	Q_s (kg/s)	Base Level Rise Rate (mm/h)	Average Delta Top Area (m ²)	Amount of Cohesive Polymer
TDB-10-1	78.2	0.451	0.011 L/s	5	4.8	0 g/120 lb of mix
TDB-12	900	0.39	3.9×10^{-4}	0.25	1.4	80 g/120 lb of mix
TDB-13-S2	700	0.39	3.9×10^{-4}	0.25	1.9	40 g/120 lb of mix

Table 2. Channel Length Scales and Mobility

Experiment	H_c (l) (mm)	B (mm)	T_c (hr)	T_{ch} (hr)	T^*
TDB-10-1	18	203	3.6	1.1	3.3
TDB-12	21.2	54	84.9	50.5	1.7
TDB-13-S2	27.3	68	109.4	45	2.4

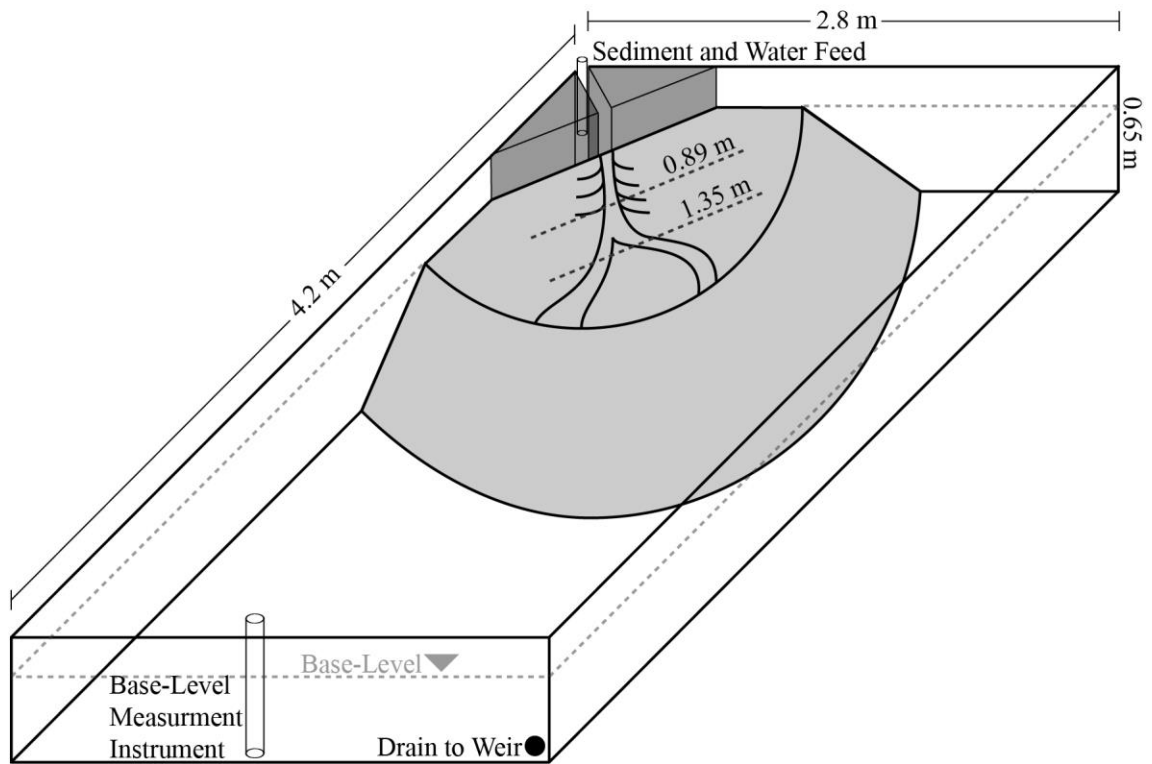


Figure 1. Schematic diagram of Tulane Delta Basin set up for the TDB-12 and TDB-13-S2 experiments featured in this thesis. The proximal transect is 0.89 m from the entrance at its center. The distal transect is 1.35 m from the entrance at its center. For the TDB-10-1 experiment the entrance was centered on the narrow wall, on the far end of the basin from the drain, and the transect of interest was located 1.63 m away from the entrance condition.

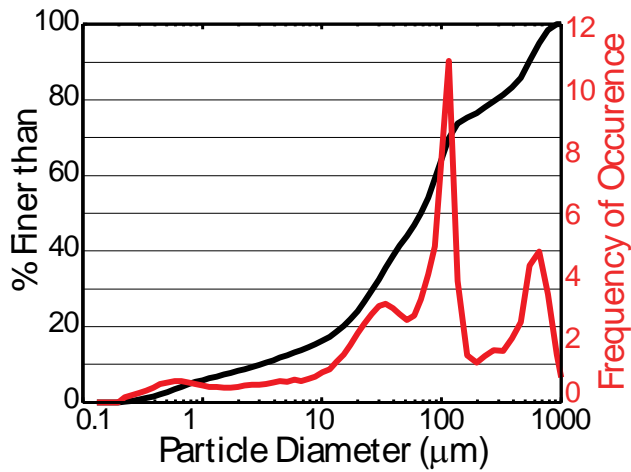


Figure 2. Grain size distribution used in the cohesive experiments. This mixture is a slightly modified version of a mixture developed at ExxonMobil and reported on by Hoyal and Sheets (2009).



Figure 3. Physical stratigraphy of the highly cohesive delta at the proximal transect. Ruler at the bottom of the image has white and orange sections that are 10 cm long for scale. The color card in the bottom of the image provides a reference for color. Coarse sediment is colored red. The blue tint in the light sediment is from the dye used to color the input water.

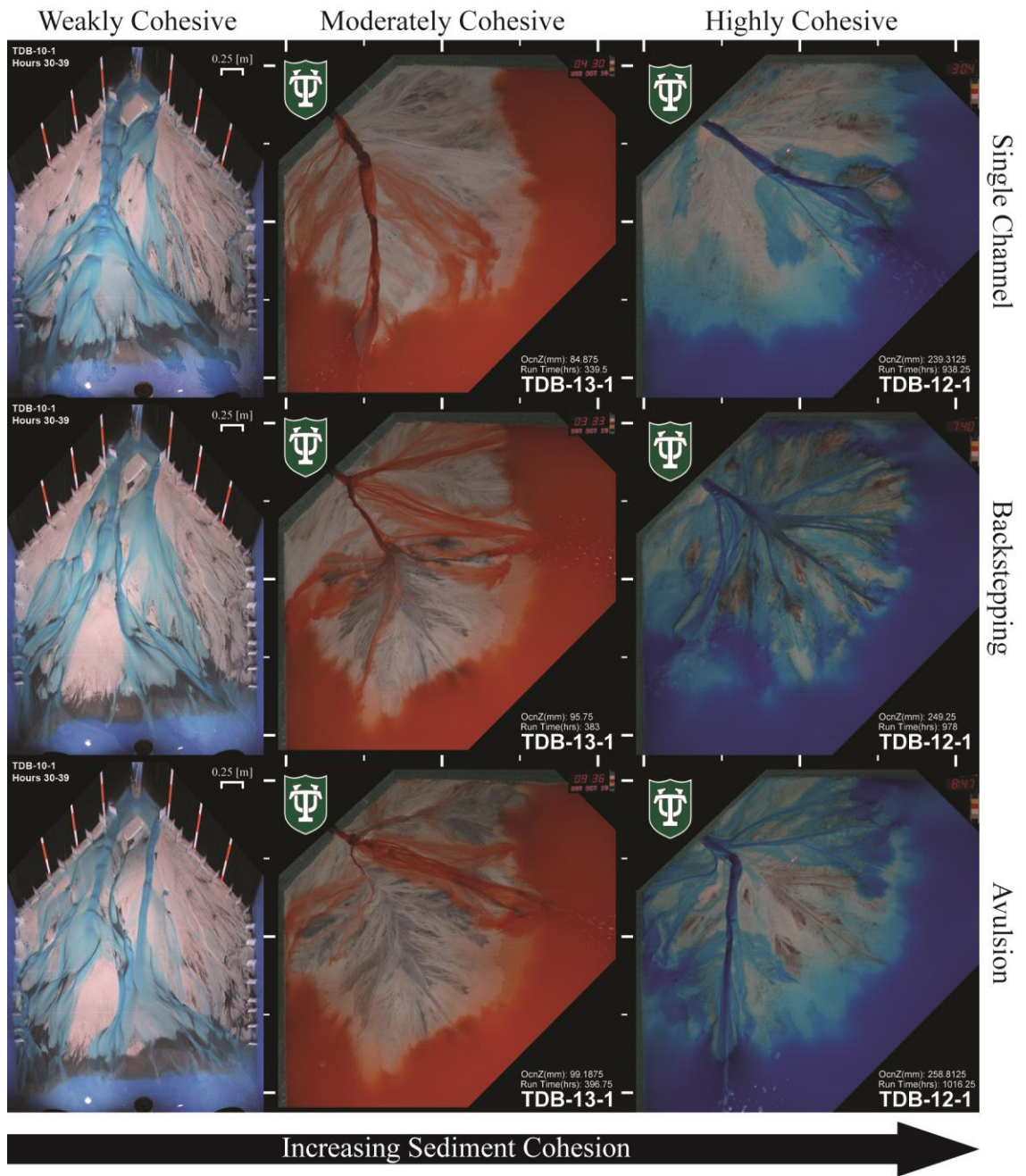


Figure 4. Overhead photographs of the three experiments. Each experiment experienced a similar process of autogenic channel formation, back stepping, and avulsion. As cohesion increased this process occurred over longer time scales, channel mobility decreased, and shoreline variability increased.

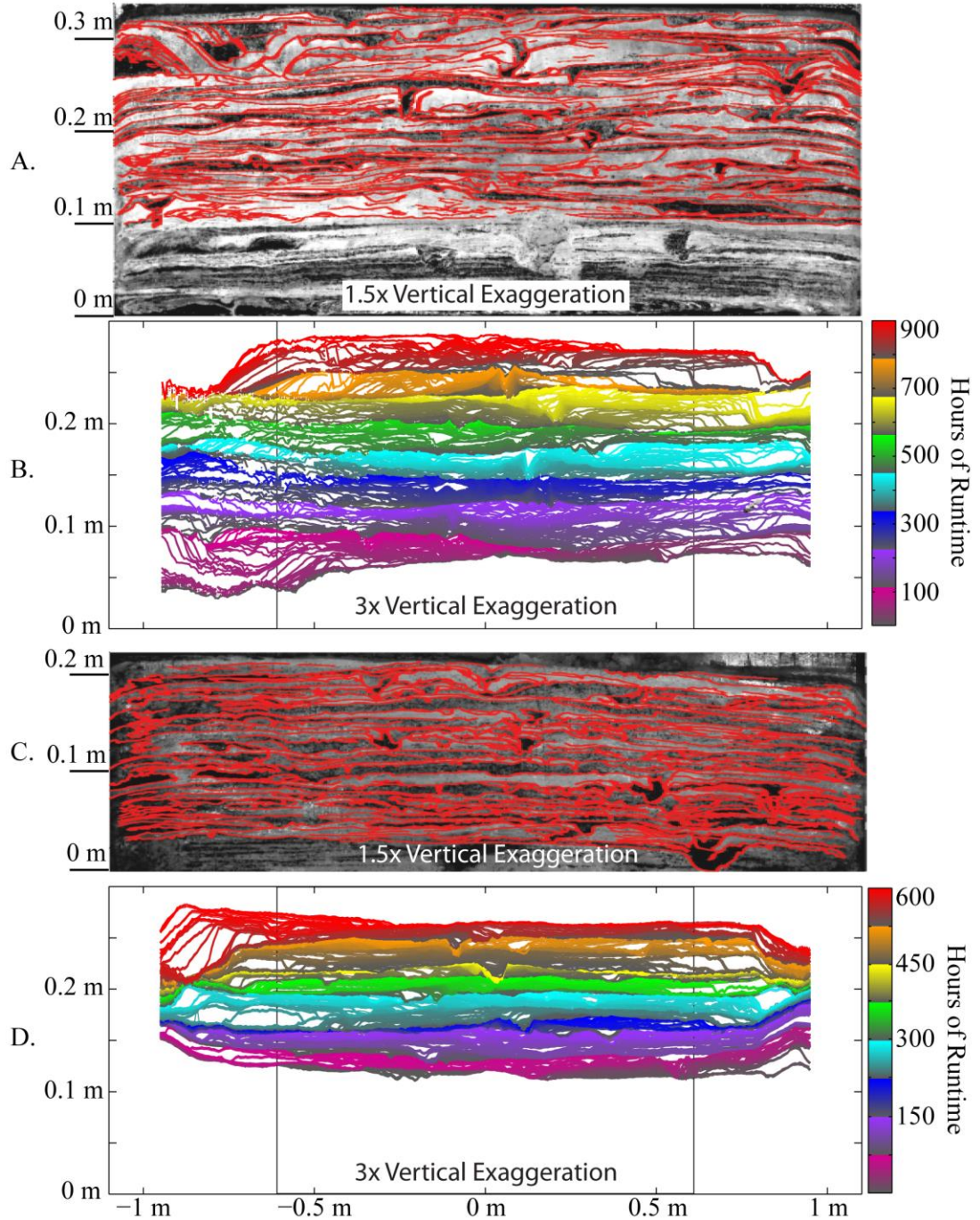


Figure 5. Physical and synthetic stratigraphic panels from experiments TDB-12 and TDB-13-S2. Vertical line within panels B, and D represent the extent of what is seen in A and C. A. Physical stratigraphy of TDB-12 with red lines highlighting handpicked stratigraphic surfaces. B. Synthetic stratigraphic cross section of TDB-12. Surfaces collected each hour from along the proximal transect. C. Physical stratigraphy of TDB-13-S2 with red lines highlighting handpicked stratigraphic surfaces. D. Synthetic stratigraphic cross section of TDB-13-2. Surfaces collected each hour from along the proximal transect.

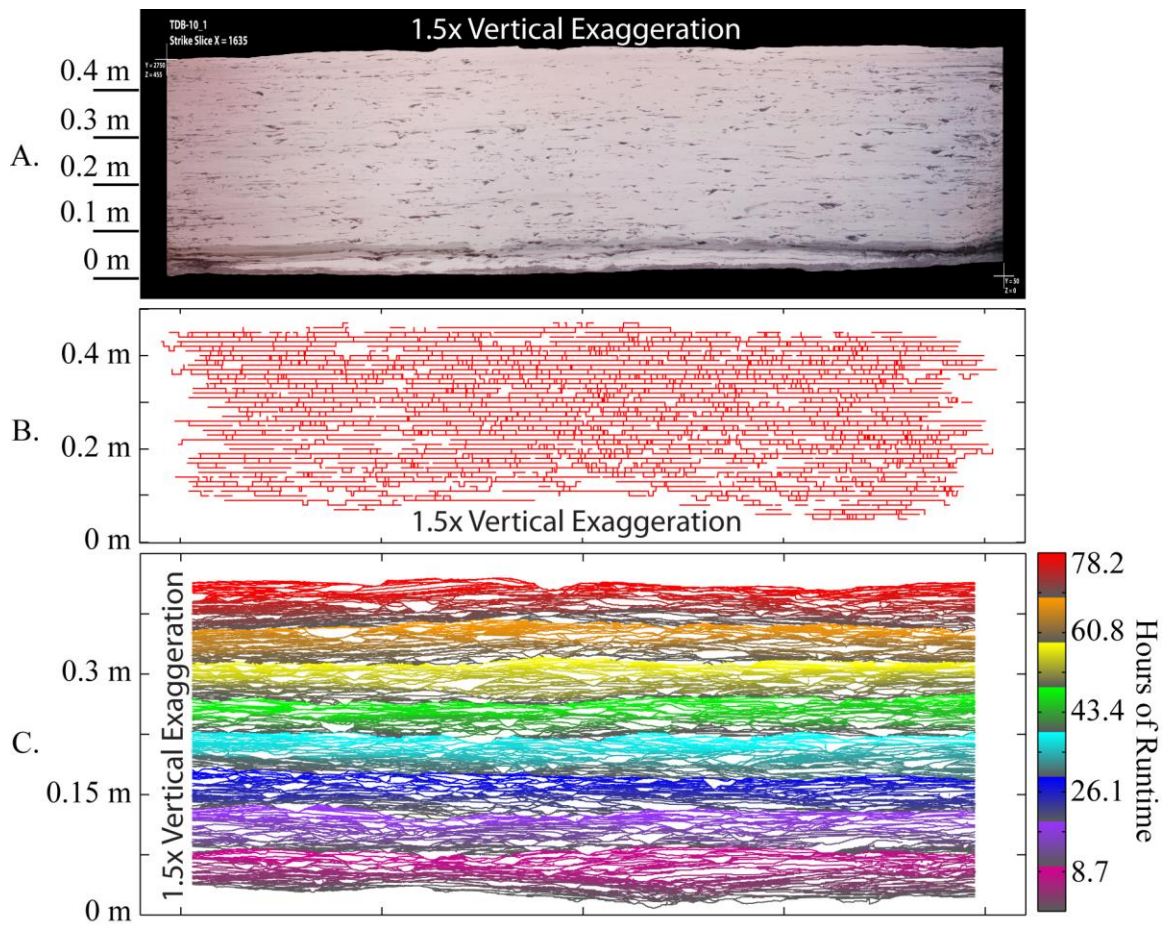


Figure 6. Physical and synthetic stratigraphic panels from experiment TDB-10-1. A. Composite image of physical stratigraphy of TDB-10-1 proximal transect. B. Red lines highlighting handpicked stratigraphic surfaces of the physical stratigraphy of TDB-10-1. C. Synthetic stratigraphic cross section of TDB-10-1. Surfaces collected every 2 minutes from along the proximal transect. The panel does not represent full width of A because the edges have been removed to minimize the influence of basin edge effects on data.

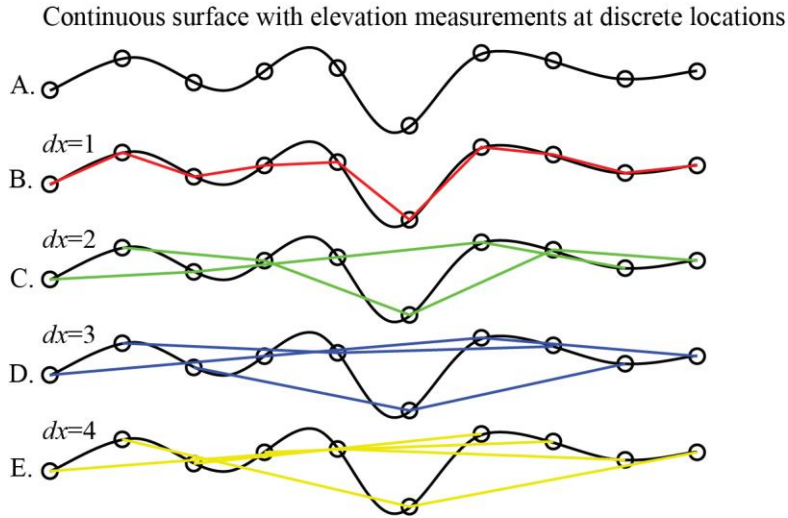


Figure 7. Method for measurement of slope as a function measurement window. Measurements of slope are collected between discrete locations along a continuous surface. The absolute values of these measurements are then averaged with the other values of the same window size. A. Continuous surface with elevation measurements at discrete locations. B. The red line connects the discrete locations using a measurement window (dx) of 1. This connects every neighboring discrete location along the continuous surface. C. The green line connects the discrete locations using a measurement window (dx) of 2. This connects all combinations of every other neighboring discrete location along the continuous surface. D. The blue line connects the discrete locations using a measurement window (dx) of 3. This connects all combinations of every third neighboring discrete location along the continuous surface. E. The yellow line connects the discrete locations using a measurement window (dx) of 4. This connects all combinations of every fourth neighboring discrete location along the continuous surface.

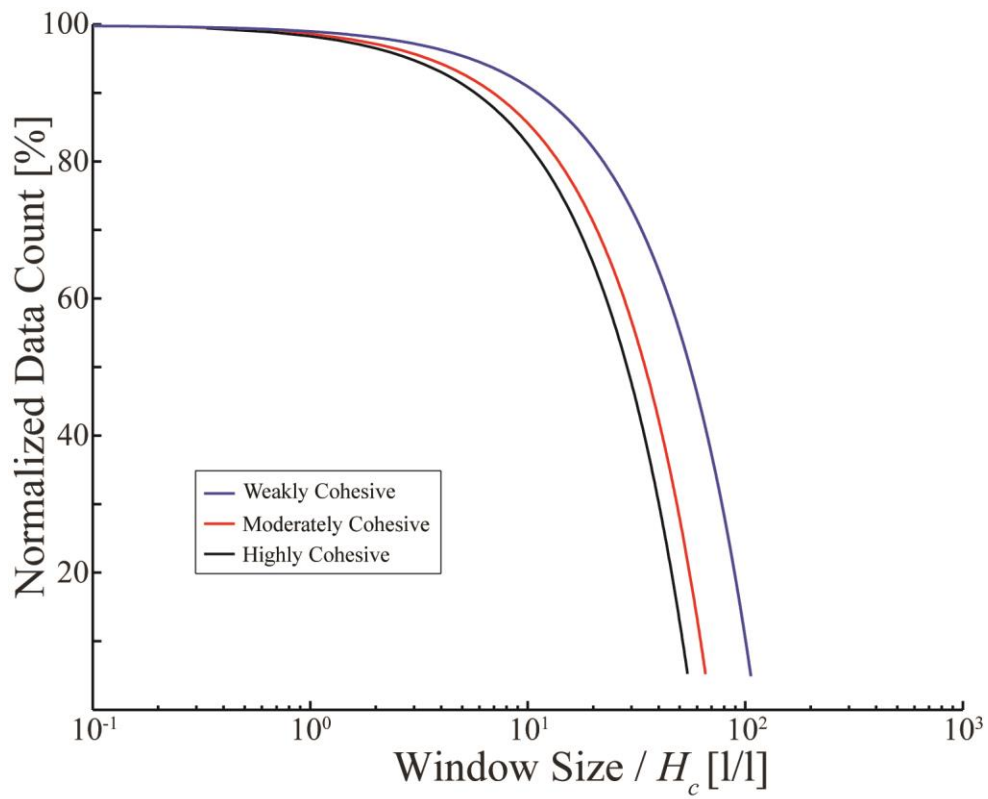


Figure 8. Normalized count of slope measurements as a function of normalized window size for topographic surfaces. Count of slope measurements is normalized by number of slope measurements at a minimum window size, while window size is normalized by H_c .

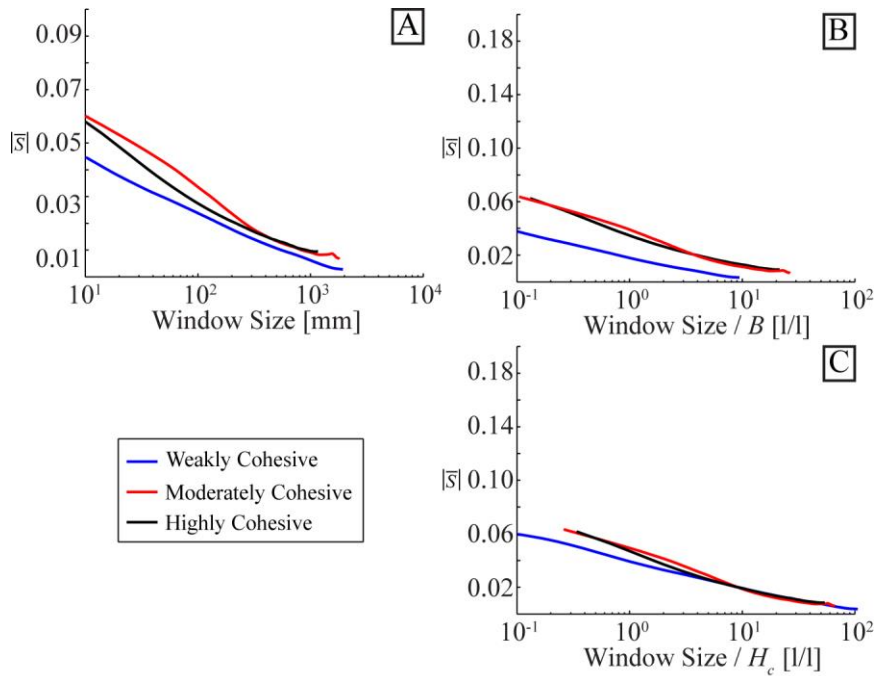


Figure 9. Mean absolute slope of topographic surfaces as a function of window size in dimensional and nondimensional space. A. Mean absolute slope of topographic surfaces as a function of window size. B. Mean absolute slope of topographic surfaces as a function of window size normalized by measured channel widths. C. Mean absolute slope of topographic surfaces as a function of window size normalized by calculated channel depths.

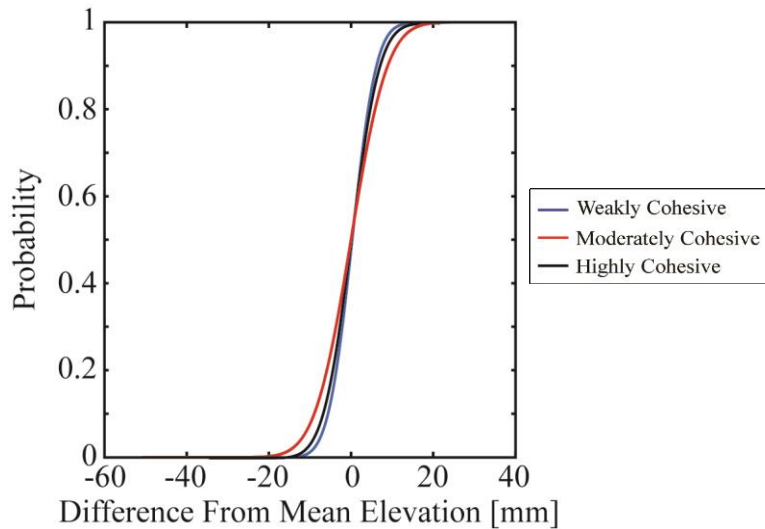


Figure 10. CDF of elevation deviations from the mean. Lower values are representative of channel bottom elevations. Higher values are representative of levee bank elevations.

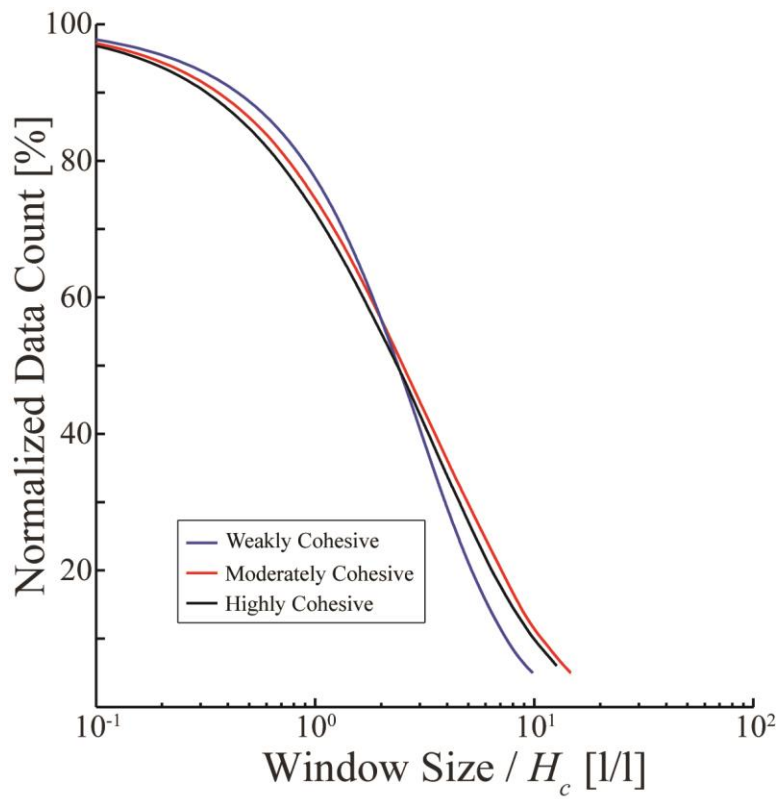


Figure 11. Normalized count of slope measurements as a function of normalized window size for physical stratigraphic surfaces. Count of slope measurements is normalized by number of slope measurements at the minimum window size, while window size is normalized by H_c .

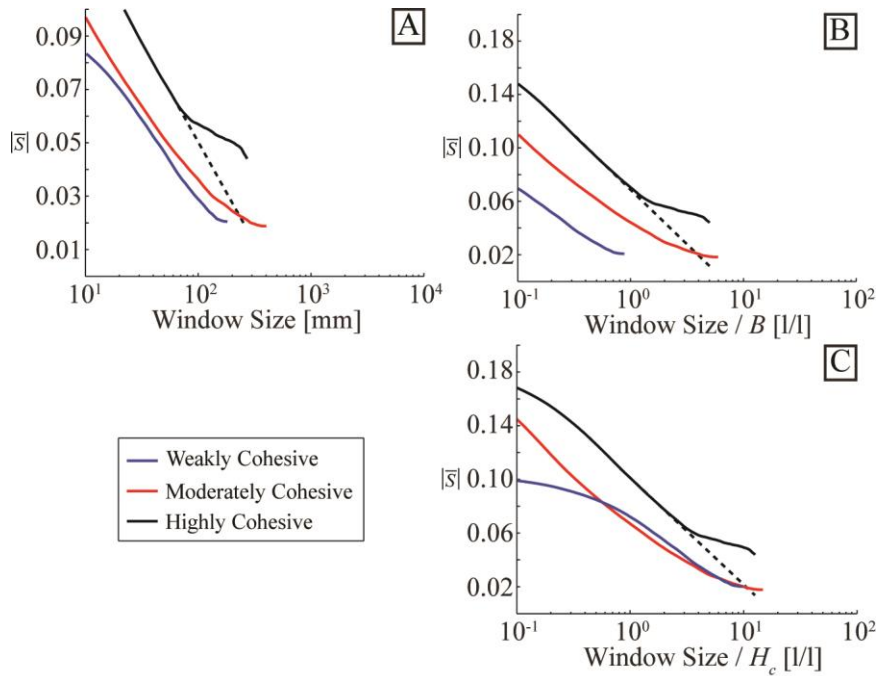


Figure 12. Mean absolute slope of stratigraphic surfaces as a function of window size in dimensional and nondimensional space. Black dotted line extends the trend of the highly cohesive delta's $\overline{|s|}$ decay. A. Mean absolute slope of stratigraphic surfaces as a function of window size. B. Mean absolute slope of stratigraphic surfaces as a function of window size normalized by measured channel widths. C. Mean absolute slope of stratigraphic surfaces as a function of window size normalized by calculated channel depths.

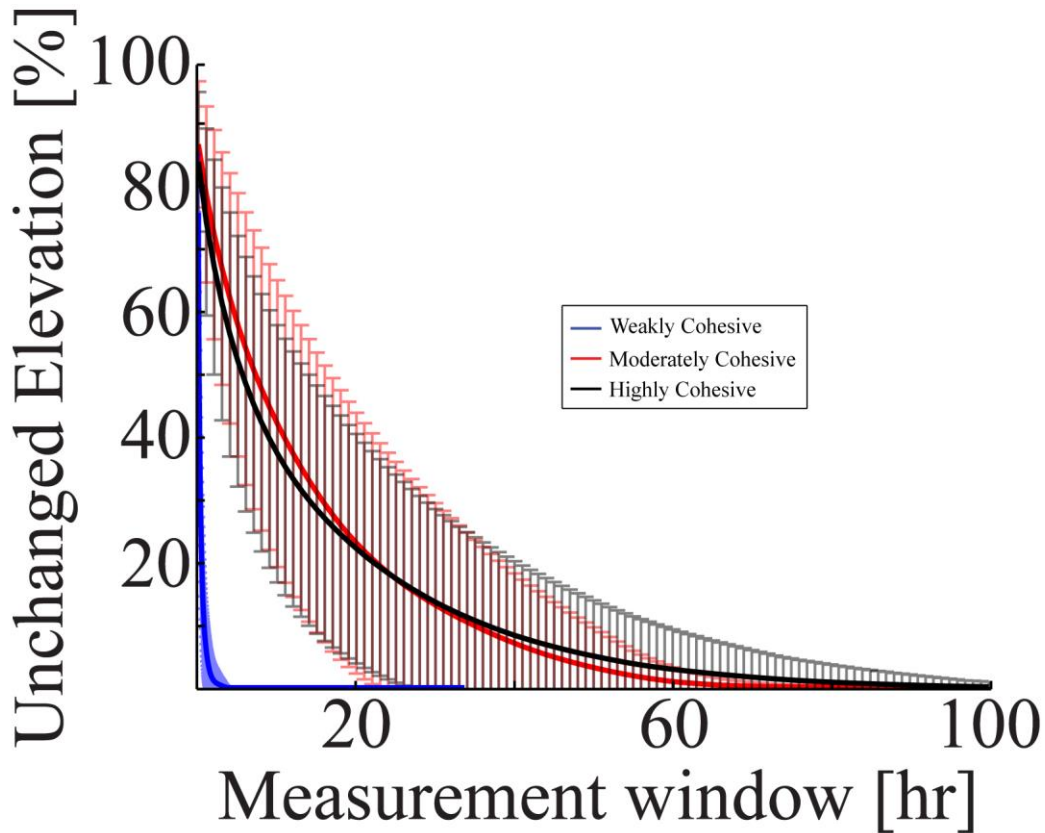


Figure 13. Data defining the reduction locations along the proximal transects that have not experienced measurable topographic change. The bold lines are the mean of the three data sets. Vertical bars are defined by +/- one standard deviation from the mean and display the variability present within the data sets.

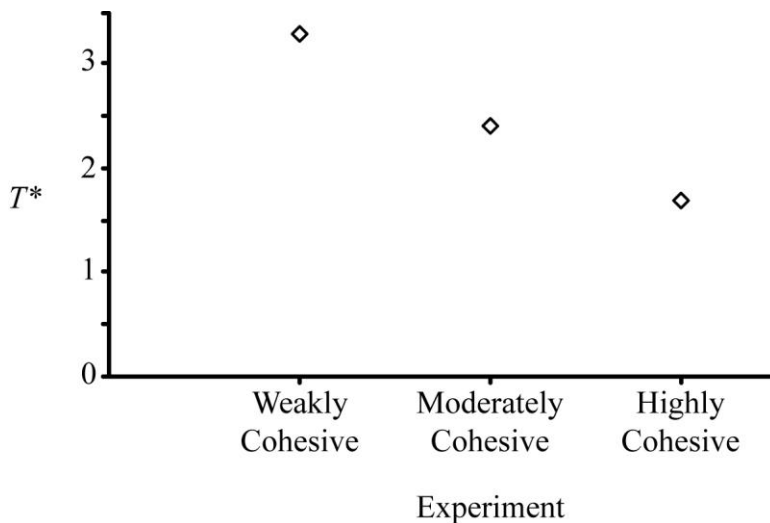


Figure 14. Normalized value of channel mobility for the weakly cohesive, moderately cohesive, and highly cohesive experiments. The value of T^* is calculated as the average time to experience measurable (1 mm) elevation change across 95% of the delta top (T_{ch}) divided by the compensation timescale (T_c).

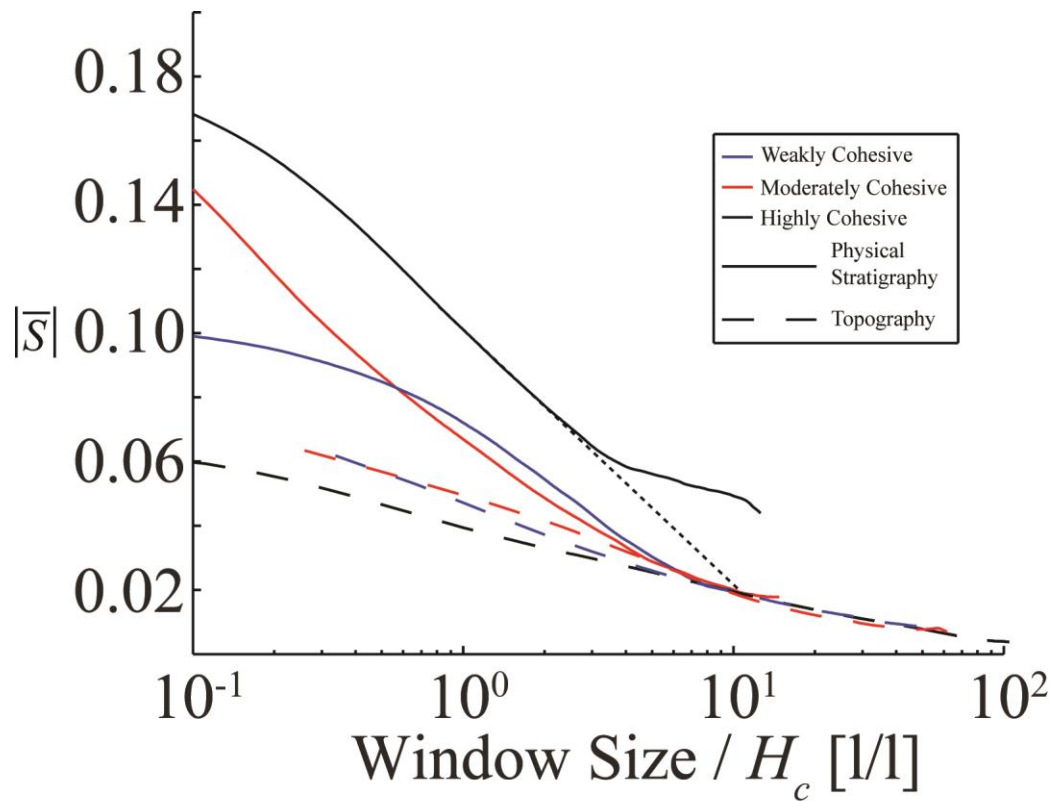


Figure 15. Mean absolute slope of physical stratigraphic surfaces (higher $|\bar{s}|$), and topographic surfaces (lower $|\bar{s}|$) as a function of normalized window size. The black dotted line extends the trend of the surface statistics of the highly cohesive experiment's physical stratigraphic surfaces.

LIST OF REFERENCES

- Allen, J.R.L., 1978, Studies in fluvial sedimentation: An exploratory quantitative model for the architecture of avulsion-controlled alluvial suites: *Sedimentary Geology*, v. 21, p. 129-147.
- Beerbower, J. R. (1964), Cyclothems and cyclic depositional mechanisms in alluvial plain sedimentation, paper presented at Symposium on Cyclic Sedimentation: State Geological Survey of Kansas, Bulletin.
- Blum, M. D., Törnqvist, T. E., 2000, Fluvial responses to climate and sea-level change: a review and look forward: *Sedimentology*, v. 47, p. 2-48.
- Bridge, J. S., and Leeder M. R., 1979, A simulation model of alluvial stratigraphy: *Sedimentology*, v. 26, p. 617-644.
- Bridge, J. S., 1993, Description and interpretation of fluvial deposits: a critical perspective: *Sedimentology*, v. 40, p. 801-810.
- Bridge, J.S., and Mackey, S.D., 1993a, A revised alluvial stratigraphy model, in Marzo, M., and Puigdefabregas, C., eds., *Alluvial Sedimentation: International Association of Sedimentologists Special Publication 17*, p. 319-336.
- Bridge, J.S., and Mackey, S.D., 1993b, A theoretical study of fluvial sandstone body dimensions, in Flint, S., and Bryant, I.D., eds., *The Geological Modeling of Hydrocarbon Reservoirs: International Association of Sedimentologists Special Publication 15*, p. 213-236.
- Bryant, M., Falk, P., and Paola, C., 1995, Experimental study of avulsion frequency and rate of deposition: *Geology*, v. 23, p. 365-368.
- Cazanacli, D., Paola, C., and Parker, G., 2002, Experimental steep, braided flow: application of flooding risk on fans: *Journal of Hydraulic Engineering*, v.128, p. 322-330.
- Dunne, T., Constantine, J. A., and Singer, M. B., 2010, The role of sediment transport and sediment supply in the evolution of river channel and floodplain complexity: *Japanese Geomorphological Union Transactions*, v. 31-2, p. 156-170
- Edmonds, D. A., and Slingerland, R. L., 2010, Significant effect of sediment cohesion on delta morphology: *Nature Geoscience*, v. 3, p. 105–109.

- Galloway, W. E., 1971, Depositional systems and shelf-slope relationships in uppermost Pennsylvanian rocks of the Eastern shelf, north-central Texas Ph.D. dissertation: University of Texas at Austin, p. 116.
- Ganti, V., Lamb, M. P., McElroy, B., 2013, Quantitative bounds on orphodynamics and implications for reading the sedimentary record: *Nature Communications* 5.
- Gibling, M.R., 2006, Width and thickness of fluvial channel bodies and valley fills in the geological record: a literature compilation: *Journal of Sedimentary Research*, v. 76, p. 731–770.
- Holbrook, J.M., 1996, Complex fluvial response to low gradients at maximum regression: A genetic link between smooth sequence-boundary morphology and architecture of overlying sheet sandstone: *Journal of Sedimentary Research*, v. 66, p. 713–722.
- Holbrook, J.M., 2001, Origin, genetic interrelationships, and stratigraphy over the continuum of fluvial channel-form bounding surfaces: An illustration from middle Cretaceous strata, southeastern Colorado: *Sedimentary Geology*, v. 124, p. 202-246.
- Hoyal, D., and Sheets, B.A., 2009, Morphodynamic evolution of experimental cohesive deltas: *Journal of Geophysical Research: Earth Surface*, v. 114.
- Jerolmack, D.J., and Mohrig D., 2007, Conditions for branching in depositional rivers: *Geology*, v. 35; no. 5; p. 463-466.
- Karssenber, D. and Bridge, J. S., 2008, A three-dimensional numerical model of sediment transport, erosion and deposition within a network of channel belts, floodplain and hill slope: extrinsic and intrinsic controls on floodplain dynamics and alluvial architecture: *Sedimentology*, v. 55, p. 1717-1745.
- Kim, W., Paola, C., Swenson, J.B., and Voller, V.R., 2006, Shoreline response to autogenic processes of sediment storage and release in the fluvial system: *Journal of Geophysical Research*, v. 111.
- Kim, W., and Paola, C., 2007, Long-period cyclic sedimentation with constant tectonic forcing in an experimental relay ramp: *Geology*, v. 35, p. 331-334.
- Kim, W., and Jerolmack, D.J., 2008, The Pulse of Calm Fan Deltas: *The Journal of Geology*, v. 116, p. 315–330.
- Li, Q., 2016, Discriminating the products of allogenic forcings and autogenic processes from sediment sources to sinks, Ph.D. dissertation: Tulane University

- Li, Q., Benson, W., Harlan, M., Robichaux, P., Sha, X., Xu, K., Straub, K.M., 2017, Influence of sediment cohesion on deltaic morphodynamics and stratigraphy over basin-filling time scales, Submitted
- Leeder, M.R., 1978, A quantitative stratigraphic model for alluvium, with special reference to channel deposit density and interconnectedness, in Miall, A.D., ed., *Fluvial Sedimentology: Canadian Society of Petroleum Geologists Memoir 5*, p. 587-596.
- Mackey, S.D., and Bridge, J.S., 1992, A revised fortran program to simulate alluvial stratigraphy: *Computers & Geosciences*, v. 18, p. 119-181.
- Mackey, S.D., and Bridge, J.S., 1995, Three-Dimensional Model of Alluvial Stratigraphy: Theory and Application: *Journal of Sedimentary Research*, v. 65B, p. 7-31.
- Mark, D.M., and Aronson, P.B., 1984, Scale-dependent fractal dimensions of topographic surfaces: An empirical investigation, with applications in geomorphology: *Mathematical Geology*, v. 16, p. 671-683.
- Martin, J., Paola, C., Abreu, V., Neal, J., Sheets, B., 2009, Sequence stratigraphy of experimental strata under known conditions of differential subsidence and variable base level: *AAPG Bulletin*, v. 93, p. 503–533.
- Niemann, J.D., Gasparini, N.M., Tucker, G.E., Bras, R.L., 2001, A quantitative evaluation of Playfair’s law and its use in testing long-term stream erosion models: *Earth Surface Processes and Landforms*, v. 26, p. 1317-1332.
- Paola, C., Straub, K., Mohrig, D., and Reinhardt, L., 2009, The “unreasonable effectiveness” of stratigraphic and geomorphic experiments: *Earth-Science Reviews*, v. 97, p. 1-43.
- Posamentier, H.W., Jervey, M.T., and Vail, P.R., 1988, Eustatic controls on clastic deposition. I. Conceptual framework. In Wilgus, C.K., Hastings, B.S., Kendall, C.G.St.C., Posamentier, H.W., Ross, C.A., Van Wagoner, J.C. *Sea-level changes: an integrated approach*, SEPM Special Publication, v. 42, p. 110–124.
- Powell, E. J., W. Kim, and T. Muto, 2012, Varying discharge controls on timescales of autogenic storage and release processes in fluvio-deltaic environments: Tank experiments, *J. Geophysical Research*, 117, F02011.
- Reitz, M.D. and Jerolmack, D.J., 2012, Experimental alluvial fan evolution: Channel dynamics, slope controls, and shoreline growth, *Journal of Geophysical Research: Earth Surface*, 117(F2).

- Rosgen, D.L., 1994. A classification of natural rivers. *Catena*, 22(3), p. 169-199.
- Sadler, P.M., 1981, Sediment accumulation rates and the completeness of stratigraphic sections: *Journal of Geology*, v. 89, p. 569–584.
- Sheets, B.A., Paola, C., and Kelberer, J.M., 2008, Creation and preservation of channel form sand bodies in an experimental alluvial system, in Nichols, G., Williams, E., and Paola, C., eds., *Sedimentary Processes, Environments and Basins: A Tribute to Peter Friend*, International Association of Sedimentologists, Special Publication 38, p. 555–567.
- Straub, K. M., and Esposito, C.R., 2013, Influence of water and sediment supply on the stratigraphic record of alluvial fans and deltas: Process controls on stratigraphic completeness: *Journal of Geophysical Research*, v. 118, p. 625-637.
- Straub, K. M., Paola, C., Kim, W., Sheets, B., 2013, Experimental investigation of sediment-dominated vs. tectonics-dominated sediment transport systems in subsiding basins, v. 83, p. 1162-1180.
- Straub, K. M., and Wang, Y., 2013, Influence of water and sediment supply on the long term evolution of alluvial fans and deltas: Statistical characterization of basin filling sedimentation patterns. *Journal of Geophysical Research: Earth Surface*, v. 118, p. 1602-1616
- Strong, N., Paola, C., 2008, Valleys that never were: Time surfaces versus stratigraphic surfaces, *Journal of Sedimentary Research*, v. 78, p. 579-593.
- Tal, M., and Paola, C., 2010, Effects of vegetation on channel morphodynamics: results and insights from laboratory experiments: *Earth Surface Processes and Landforms*, v. 35, p. 1014-1028.
- Wang, Y., K. M. Straub, and E. A. Hajek, 2011, Scale-dependent compensational stacking: An estimate of autogenic time scales in channelized sedimentary deposits, *Geology*, 39(9), 811-814.
- Wickert, A. D., Martin, J. M., Tal, M., Kim, W., Sheets, B., Paola, C., 2013, River channel lateral mobility: metrics, time scales, and controls: *Journal of Geophysical Research: Earth Surface*, v. 118, p. 396-412.

BIOGRAPHY

William “Matt” Benson was born in Columbia, South Carolina. He grew up in Charlotte, North Carolina before attending Washington and Lee University for his undergraduate degree in geology and economics. Immediately following his time in undergraduate he began graduate school, working in Tulane’s Sediment Dynamics and Quantitative Stratigraphy group. After completion of his master’s thesis he hopes to pursue a humble life of continued learning, and adventure.